This article has been accepted for publication in IEEE Open Access Journal of Power and Energy. This is the author's version which has not been fully edited and content may change prior to final publication. Citation information: DOI 10.1109/OAJPE.2023.3268499

A Practical Solution for Locating the Source of Voltage Dips in HV/MV Interconnected Grids

P. Castello, *Member, IEEE,* C. Muscas, *Senior Member, IEEE,* P. A. Pegoraro, *Senior Member, IEEE,* S. Sulis, *Senior Member, IEEE*, J. Rens, *Member, IEEE,* J. van Zyl

Abstract— Monitoring the technical performance of a power system is significantly enhanced when distributed instrumentation produces coherent field data, i.e., synchronized by GPS timestamping. In this paper a practical methodology is presented to improve the localisation of the source of a voltage dip on power grids. The proposed solution makes use of synchronised dip data provided by power quality meters. Field data reporting events occurred in an HV/MV interconnected system in South Africa are used to validate the results obtained by the improved method and compare with results of two alternative methods.

Index Terms-- Voltage dips, Power Quality meter, field data platform, time accuracy, synchronization.

I. INTRODUCTION

Synchronized measurement devices can improve power system operations [1] thanks to the better understanding of system technical performance resulting from the comparison of field data recorded at geographically different locations. A system-wide implementation of network coherent data acquisition and hosting could be challenged by huge volumes of data, but solutions nowadays exist to acquire, store, and analyse big data [2], [3].

Accurate timestamping, like the 1 μs requirement of the IEC 60255-118-1 [4] synchrophasor measurement standard, increasingly finds application in power system instrumentation such as in Power Quality meters (PQM). This capability presents, amongst others, the opportunity to improve voltage dip localisation. This is being explored in this paper.

Because time reference is absolute when using GPS, field data from different types of instruments can be directly compared. As example, data produced by digital fault recorders (DFRs) and PQMs [5], [6] can be simultaneously analysed [7], [8].

Synchronisation accuracy has to be at least in the order of milliseconds when a PQM is certified compliant to the Power Quality (PQ) measurement requirements of IEC 61000-4-30 Class A, edition 3 (and soon, edition 4) [9]. This allows voltage events recorded at different points in an interconnected network to be aggregated into a single network incident by grouping events sharing a close timestamp. A single root-cause can be the reason for a number of voltage events (such as dips) recorded at the same time, but at different locations.

A voltage event trigger is based on a least a ½-cycle sliding observation of the RMS voltage (IEC 61000-4-30 requirement). The consequence is that a voltage dip event needs to last for longer than 10 ms (50 Hz) or 8.333 ms (60 Hz) to be classified as a voltage dip event ("dip" and "sag" are interchangeable terms).

Recent updates of the IEEE 1159.3-2019 data transfer standard [10] allow software platforms to host and analyse data from instruments of different manufacturers. The same data repository can be used. Voltage dip analysis is one aspect of power system operations to benefit.

Wide-area measurement systems (WAMSs) use phasor measurement units (PMUs), producing the synchrophasors needed in the estimation of the grid state. A high reporting rate and high levels of timestamping accuracy [11] allow WAMSs to correlate events detected at different nodes of the grid. PQ data analysis can benefit from additional PMU data as timestamping of parameters of interest, obtained from different sources, is now absolute.

Of interest in this paper is identifying the geographical origin of voltage events, which, in turn, permits assigning responsibility to the operator of that network for causing the disturbance. In this scenario, the goal is not deriving the location exactly, but identifying a section of the network as the host of the root-cause. Voltage dips are the result of mostly fault currents and if the knowledge exist on how the protection in that section of the network has contained the fault current, then the root-cause of the voltage dip can be identified.

On this basis, network operators can devise complimentary mitigation solutions to further improve the voltage dip performance of their network.

Detection, analysis and classification of voltage dips are well-known topics in PQ studies and have been discussed in scientific literature (see for example, [13]-[15]). Different algorithms can be considered to derive direction, that is to determine if the voltage dip is upstream or downstream from

Dr. Castello's work was partially supported by "Convenzione triennale tra la Fondazione di Sardegna e gli Atenei Sardi - Regione Sardegna L.R.7/2007 DGR DGR 28/21 with project "Formal Methods and Technologies for the Future of Energy Systems", F72F20000350007, call 2019

P. Castello, C. Muscas, P. A. Pegoraro and S. Sulis are with the Department of Electrical and Electronic Engineering, University of Cagliari, Cagliari, Italy (email: paolo.castello@unica.it).

J. Rens, is with the School for Electronic and Electrical Engineering North-West University Potchefstroom, South Africa USA (e-mail: johan.rens@nwu.ac.za).

J. van Zyl is with the CT LAB Bietigheim-Bissingen, Germany (e-mail: jacobus@ctlab.com).

This work is licensed under a Creative Commons Attribution 4.0 License. For more information, see https://creativecommons.org/licenses/by/4.0/

This article has been accepted for publication in IEEE Open Access Journal of Power and Energy. This is the author's version which has not been fully edited and content may change prior to final publication. Citation information: DOI 10.1109/OAJPE.2023.3268499

the measurement point. A set of Boolean logics are used in [16] to track power flow during symmetrical and asymmetrical voltage dips to identify the direction of the voltage dip source. In [17], voltage information only is considered to identify the source of the voltage dip as being in the network connected to the primary or to the secondary sides of a transformer. It considers pre-fault voltages and the residual voltages during the voltage dip taking into account the grounding scheme (i.e., star not grounded/star grounded). Machine learning and signal processing is integrated in [18] and [19] in finding the source of the voltage dip. These solutions can handle huge amounts of data. Implementation of the above methods requires in-depth knowledge of power system operation and the mathematical implementation in customised software.

The approach proposed in this paper addresses practical needs expressed by different grid operators, and in particular that of localising the origin of voltage dips between different voltage levels in the same network under investigation, mostly medium voltage (MV) and high voltage (HV). In this paper, a simple but practical and efficient method for automatic identification of voltage source direction is then presented. Only basic parameters such as residual voltage, duration and start time of event, need to be considered.

Two methods for identifying voltage dip sources will be first analysed ([20], [21]). They are based exclusively on the measurements provided by the PQMs, aiming at a simple data management. Then, after outlining the possible limits of such approaches, the new method is proposed, which improves voltage dip source identification performance. The improved method is also able to integrate additional measurements, such as from a HV system. Data obtained from real synchronised PQMs are used. Validation is indeed performed on field data provided by a distributed measurement system in Southern Africa [22].

First, in Section II, existing methods that aims to derive the source of a voltage dip are presented. Section III then presents the new improved methodology. Section IV presents the used data platform while Section V validates the proposed method using field data and compares the results with those obtained by the methods described in Section II.

II. Identification of Voltage Dips Sources

Voltage dips in MV distribution grids can be due to either normal grid operations (such as energization of transformers and starting of motors) or unplanned causes such as short circuits caused by vegetation, atmospheric phenomena (e.g., lightning) and equipment failure. They may originate in the local MV grid, in end-user plants or in an interconnected HV grid.

A meshed topology can cause a single network incident at HV to result in a number of voltage dip events at different MV substations, even far away [23]. Therefore, specific techniques are needed to further a global understanding of where in the network that root-cause is located and what the reason to an increase in current was (such as a single-line to earth fault caused by lightning, vegetation, and others). This knowledge set then helps system operators to intervene, and over time, to improve network dip performance.

For instance, a goal of the Italian PQ monitoring system is to identify in which HV or MV network the dip incident originated. Data analysis of dip data recorded by the QuEEN monitoring system (details in [24] and [25]) during 2010-2014 showed that the percentage of dip events recorded at MV attributable to faults in the HV network is about 40% of the total events recorded at MV.

Most of the time, the deepest dip event should be the nearest to the root-cause as the impedance between the point where the dip was recorded, and the point where the fault occurs will be the lowest, resulting in the lowest residual voltage (product of current and impedance). This is understood, by considering how fault level allows approximation of the residual voltage during a network fault, using (1) below:

$$V_{sag} = 1 - {}^{S_{Fault}}/_{S_{PCC}} \quad (1)$$

where:

- V_{sag}: Residual voltage in p.u. at the Point of Common Coupling (PCC) during a fault at a (mostly) downstream point in the network.
- S_{PCC}: Fault level (apparent power) at a node considered as a PCC in the network under observation.
- S_{Fault}: Fault level (apparent power) at the point where the maximum depth of a voltage dip is to be estimated. This fault level is different from S_{PCC} due to a transformer and/or line between the position of the fault and the PCC.

It is evident from (1) that the potential exists to have a zero residual voltage at the PCC if a zero-impedance fault occurs at that PCC. Mostly the fault will be some electrical distance away, resulting in a larger than zero residual voltage.

Voltage dips originating from higher voltage levels are normally deeper compared to voltage dips originating from a lower voltage level, as the voltage drop towards a higher voltage level is reduced by the additional impedance of transformers between the fault and the measurement.

The duration of a dip event could be different between different events belonging to the same disturbance incident. A different slope of the RMS profile of the dip event during the start and end of the dip at one location compared to the slope of the RMS profile at another location is common. Normally, the slope at the site located nearest to the root-cause is the steepest. Deeper into the network, the slope will be less steep due to local reactive power support.

Rotating loads at a specific point in the network will accelerate during the end of the dip event as voltage starts to rise. This is to regain inertia that was lost when voltage was reduced during the dip event. Acceleration requires a current inrush consequently causing a reduced rate of voltage recovery resulting from the voltage drop across the impedance between the accelerating rotating load and the measurement point.

The above features support the development of techniques aimed at identifying the portion of the grid where a voltage dip originates using the most basic dip data.

Next, two different methods [20], [21] that estimate if a voltage dip originated in the upstream (e.g., HV) or downstream

This work is licensed under a Creative Commons Attribution 4.0 License. For more information, see https://creativecommons.org/licenses/by/4.0/

This article has been accepted for publication in IEEE Open Access Journal of Power and Energy. This is the author's version which has not been fully edited and content may change prior to final publication. Citation information: DOI 10.1109/OAJPE.2023.3268499

(e.g., MV) system are analysed. Referred to as method M1 and method M2, respectively, their theoretical principles are considered.

In order to deal with the possible presence of asymmetrical voltage dips, the methods provided by [9] for the classification of this kind of events are used in this paper: a dip begins when the RMS voltage of one or more channels is below the dip threshold and ends when the RMS voltage on all measured channels is equal to or above the dip threshold plus the hysteresis voltage; the residual voltage of a voltage dip is the lowest RMS value measured on any channel during the dip.

Method M1

Method M1 (hereafter briefly M1) was proposed by the Italian Authority of energy in Directive 198/2011 [21]. It can be applied to a voltage incident comprising of a number of voltage dips simultaneously detected on the MV busbars of the same HV/MV substation. M1, as defined in [21], can only be applied to one substation at a time.

Assume that a voltage dip originates in a HV network and is detected at all MV busbars supplied from the same HV busbar in a single substation using the network configuration shown in Fig. 1 below.

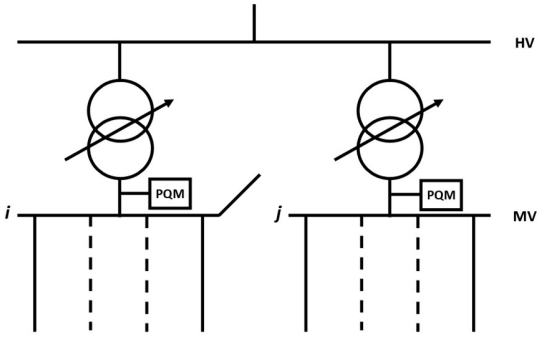

Fig. 1. Single substation with two HV/MV transformers.

The origin of all voltage dip events measured at the same time is attributed to the HV grid if all three following conditions are satisfied (the formulation considers only two voltage dip events at two MV busbars, but it can be easily extended to more events):

1. Residual voltages of the voltage dip events differ by no more than 3 %.

$$\Delta V = |V_i - V_j| \leq 3\ \% \quad (1)$$

where V_i and V_j are the RMS values of the residual voltages (normalized to percentage) of voltage dip events recorded at the same time in MV busbars i and j, respectively. Different threshold values can be configured; for instance in [26], a threshold value of 10 % is used. This condition is intended to check for similarity in event depths (or residual voltages).

2. Voltage dip events occur within 60 ms of each other.

$$\Delta T = |T_i - T_j| \leq 60\ \text{ms} \quad (2)$$

where T_i and T_j are the timestamps of the considered voltage dip events. This condition considers “simultaneous" events.

3. Duration of considered voltage dip events are within 20 ms of each other.

$$\delta t = |\Delta t_i - \Delta t_j| \leq 20\ \text{ms} \quad (3)$$

where Δt_i and Δt_j are the durations of the considered voltage dip events recorded in MV busbars i and j. Condition (3) aggregates events sharing a similar duration as they should also share a similar root-cause.

Method M2

Method M2 (hereafter briefly M2) has been proposed in [20] to analyse voltage dip events detected at almost the same time but at different MV busbars in different HV/MV substations. They are electrically close by sharing the same HV supply, as shown in Fig. 2 below.

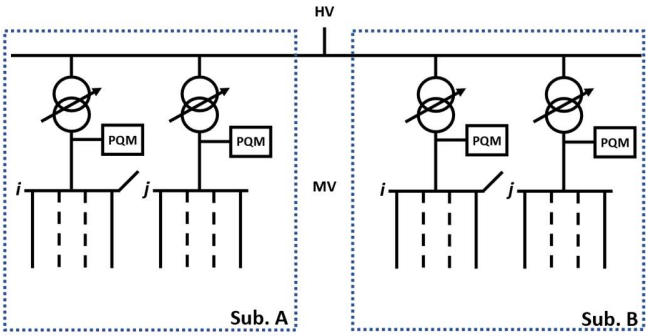

Fig. 2. Two substations (Sub. A and Sub. B) on the same HV line

M2 considers only one condition; namely, the origin of the voltage dip events is attributed to the HV grid if the recorded dip events occur within 60 ms of each other:

$$|T^A - T^B| \leq 60\ \text{ms} \quad (4)$$

where T^A and T^B are the timestamps of the voltage dip events at a generic MV busbar of the HV/MV substations A and B, respectively, fed by the same HV network.

In scientific and technical literature different values have been proposed for the voltage and time thresholds used in the above two methods. For residual voltage in (1), a ΔV threshold from 3 % to 10 % is used. The time difference on the starting time of the dip trigger in (2) and (4) is set to either 60 ms or 70 ms [26]. The threshold in the difference in dip duration δt used in (3) is set to 20 ms, but in other papers in the literature it is up to 500 ms. Specific values for the threshold voltage and time values should reflect the conditions in the grid under investigation. In this paper, the threshold values considered in [20] are used.

III. Improved Localisation of Voltage Dips

The limitations in M1 and M2 are discussed below as the context to why the proposed method (indicated as M3) performs better.

1) Method M3

Application of M1 and M2 on a power system may result in limited performance in some circumstances. M1 requires that all dips are measured at a single substation. The performance of M2 is affected when a dip event originates on the MV side of

This work is licensed under a Creative Commons Attribution 4.0 License. For more information, see https://creativecommons.org/licenses/by/4.0/

This article has been accepted for publication in IEEE Open Access Journal of Power and Energy. This is the author's version which has not been fully edited and content may change prior to final publication. Citation information: DOI 10.1109/OAJPE.2023.3268499

one substation and then detected (with higher residual value) on the MV busbar(s) of a nearby substation. M2 could then mistakenly attribute the origin of this network dip incident to the HV network.

M3 first merges the criteria of M1 and M2 by analysing a network dip incident using a criterion similar to (4) and then complementing it by a residual voltage requirement similar to (1).

The same network topology in Fig. 2 is considered to evaluate M3. When a voltage dip is detected at two different MV busbars of HV/MV substations sharing the same HV supply, the dip events are grouped into a single incident if the difference between the dip trigger timestamps at each MV busbar is sufficiently small:

$$\left|T^A - T^B\right| \leq \Delta T_{start} \quad (5)$$

When the time difference is less than ΔT_{start}, it is assumed that they most probably share a root-cause.

The voltage dip incident is attributed to the HV grid if the following condition is met:

$$\left|V^A - V^B\right| \leq \Delta V_{lim\%} \quad (6)$$

where V^A and V^B are the RMS values (in percent) of the residual voltages of the two voltage dips simultaneously recorded in MV busbars of substations A and B, respectively. If the voltage difference in (6) is higher than the limit value ($\Delta V_{lim\%}$), then the origin of the voltage dip incident is in the section of the MV grid where the lowest residual voltage value was measured.

Monitoring, not necessarily in exact coherence, all branches in the MV grid maximises the ability of M3 to precisely locate the origin of the voltage dip, similar for M1 and M2. However, in order to improve the reliability of M3, the method can exploit the availability of synchronous dip data from the HV grid as provided by PMUs or PQMs. In this case, the dip incident is attributed to the HV network if the following criteria are simultaneously fulfilled:

$$\max\{\left|T^{HV} - T^A\right|, \left|T^{HV} - T^B\right|\} \leq \Delta T_{start} \quad (7)$$

$$\left|V^{HV} - V^X\right| \leq \Delta V_{lim\%} \quad (8)$$

where V^{HV} is the residual RMS voltage (in percent) of the voltage dip recorded in the HV grid and, in V^X, the superscript X can be either A or B. If the voltage difference in (8) is more than the limit value ($\Delta V_{lim\%}$) for a given X, then the origin of the voltage dip incident is attributed to the section of the MV grid supplied by the corresponding busbar.

The threshold values for voltage and time differences can be configured according to the specific grid conditions, reflecting the monitoring strategy pertaining to a specific network.

As described in [20], the on-load tap-changers at the HV/MV transformers can be in different positions, resulting in ΔV exceeding the 3% limit used in M1 [20]. Also, when hosting significant distributed renewable power generation, power flow through transformers can be variable [20] in magnitude and direction. To account for the above and the difference between residual voltages at different nodes, contributed by voltage drop across the impedance between one measurement point and another, the voltage threshold $\Delta V_{lim\%}$ used for M3 is set in this paper at 10 % and the timestamp difference is ΔT_{start} = 60 ms.

2) Improved solution for clustering voltage dips

Two voltage dip events at different locations, sharing the same root-cause, can have a significantly different RMS voltage profile, as shown in Fig. 3.

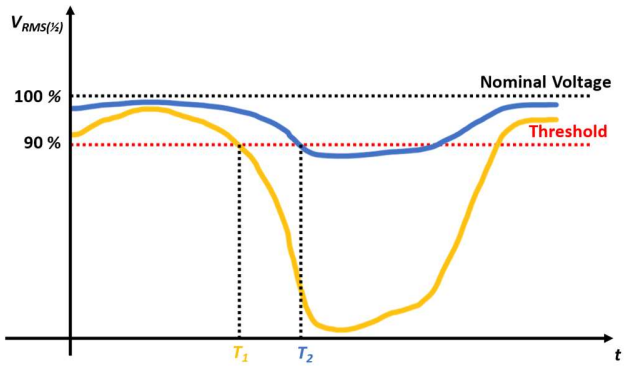

Fig. 3. Example of two RMS voltage profiles corresponding to two simultaneous dip events measured at two remote locations but having different start times (T_1 and T_2).

The yellow RMS voltage profile at the first node shows a deep and steep voltage drop during the start of the event, triggering an IEC 61000-4-30 dip condition detection at time T_1. At the second node, the blue RMS voltage profile is characterized by a higher residual voltage changing at a much lower rate and this is the reason why the trigger threshold is only exceeded at time T_2.

As a consequence, the start time difference between the two dip events may be larger than the criterion considered in (4), (5), or (7), suggesting that the two voltage dip events are unrelated, even if they are actually sharing the same root cause.

This constraint is overcome by considering an aggregation methodology that does not rely only on the absolute difference in the timestamping of different dip events. Additional details of each dip event are also analysed. If the shallower voltage dip is located within the deeper one (i.e., the start time of the shallower dip occurs after that of the deeper voltage dip, and the shallower dip ends before the deeper dip), then the two events are related to the same root-cause. In this scenario, the timestamping accuracy is important. For the above reason, an additional time difference reflecting timestamping uncertainty (e.g. ± 20 ms, for instruments compliant to IEC 61000-4-30, class A at 50 Hz [9]) must be considered for the time instants used in this criterion.

In the results presented in Section V, the improved clustering criterion presented in this section will be referred to as (5*), if only MV measurements are used, or (7*), if additional HV measurements are considered.

IV. A Dip Data Platform

Field data considered in this paper was extracted from Osprey Pro[1], a Cloud-based PQ data hosting and analysis platform.

Osprey Pro was initially developed to host PQ data produced

[1] https://otelloenergy.com

This work is licensed under a Creative Commons Attribution 4.0 License. For more information, see https://creativecommons.org/licenses/by/4.0/

This article has been accepted for publication in IEEE Open Access Journal of Power and Energy. This is the author's version which has not been fully edited and content may change prior to final publication. Citation information: DOI 10.1109/OAJPE.2023.3268499

by the Vecto 3[2], a Class A IEC 61000-4-30 (edition 3) PQ meter, but other sources and types of data (i.e., synchrophasors, energy) can be accepted.

Osprey Pro can be configured to automate the detection and matching of events. It permits adding metadata such as root-cause information on voltage waveform events (lightning, vegetation, copper theft, network operations and others).

Fig. 4 shows an example of a network dip incident resulting from the automated matching of seven dip events recorded simultaneously at different 11 kV and 66 kV nodes in Southern Africa. This allows focusing on a single network incident instead of multiple dip events.

An automated method that reliably identifies where in the network the most likely location of the root-cause is would be then useful. Waveform analysis can be included as synchronized voltage and current waveform data (with a sampling rate up to 50 kHz) are retained at each measurement point when a dip occurs.

Voltage dips analysed in this paper were detected by tracking the RMS voltage profile at a 1/6-cycle resolution compared to the ½-cycle minimum requirement of the IEC 61000-4-30. The case studies presented in the following section were analysed in depth by grid operators, which, by exploiting all the available information (measurement data, status of switches and breakers, etc.), were able to identify the source of the voltage sags. This information will be used as "ground truth" in the validation of the presented methodologies.

Next, the three localization methods (M1, M2 and M3) are applied and compared.

V. Voltage Dip Source Localization: Application

This section first considers how different dip events can be aggregated to a single network incident. The results obtained by the improved methodology M3 are then compared with the performance of M1 and M2.

1) From multiple voltage dips to a single voltage dip incident

A network voltage dip incident comprising 7 different voltage dip events at 7 different measurement points and at different voltage levels is considered. In particular, Fig. 5 presents 2 dip events recorded at 2 different 11 kV nodes of the South African grid, 20 km apart (shown as PQMs 3.9 and 4.2 in Fig. 5).

The voltage dip detected by PQM 3.9 has a lower residual voltage of 61 %, attained by an almost vertical slope leading to the dip trigger activated quicker than at PQM 4.2, where the residual voltage is higher. The dip trigger at PQM 4.2 is activated somewhat later due to the slope being less steep. Dip triggers are set at 90% of the nominal voltage at each substation.

The difference in voltage start times is more than 70 ms (76 ms to be exact). This is an example where the aggregation methodology of M1 or M2 would not have identified these two dip events as a single network dip incident, while the improved aggregation principle proposed in this paper does it.

It the case of two dips that are unrelated but measured

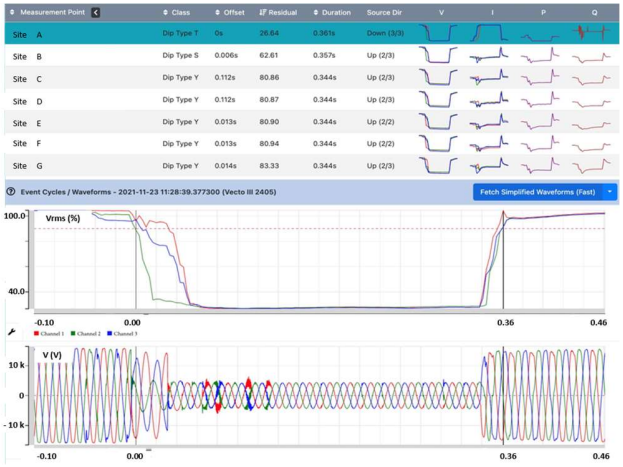

Fig. 4: Example a power quality incident within the OspreyPro platform.

simultaneously, all the above clustering methods (i.e., both the original one used in M1, M2 and the improved one used in M3) would incorrectly treat them as a single voltage dip incident. Having, in a limited area, two simultaneous dips resulting from two unrelated root-causes is however considered an event with a very low probability.

The performance of M3 is discussed in more details in the following subsection.

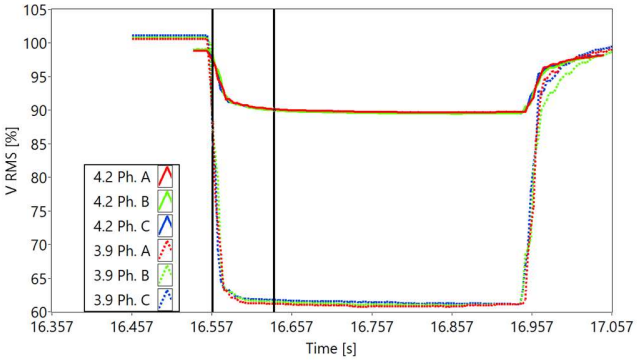

Fig. 5. RMS voltages measured at two nodes during a voltage dip.

2) Application of M3

Four case studies making use of synchronised field data within a South African grid are used to demonstrate the performance of M3 in comparison to M1 and M2. The cases reported here are a representative sample of a larger set of events that have been detected and analysed.

Three different 66/11 kV substations (Fig. 6) are considered within a large interconnected power network. They share a 66 kV line and each pair is about 6 km apart.

[2] www.ctlab.com

This work is licensed under a Creative Commons Attribution 4.0 License. For more information, see https://creativecommons.org/licenses/by/4.0/

This article has been accepted for publication in IEEE Open Access Journal of Power and Energy. This is the author's version which has not been fully edited and content may change prior to final publication. Citation information: DOI 10.1109/OAJPE.2023.3268499

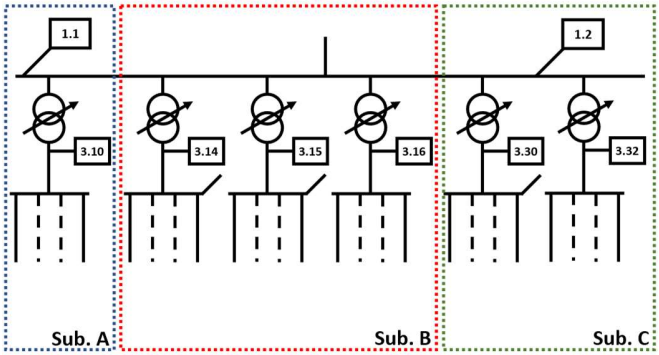

Fig. 6. Measurement devices at substations A, B and C.

A) Case Study 1

Table I lists the results obtained by M1, M2 and M3 on a network dip incident comprising 6 dip events considered "simultaneous" by the criterion (7*). In addition to the residual voltage and duration of each dip event, the time offsets of each dip event are listed in Table I. A maximum offset of 2 ms is observed.

This asymmetrical incident was detected by 4 PQMs installed on the MV busbar (PQM 3.10, PQM 3.14, PQM 3.15, and PQM 3.16) and 2 PQMs (PQM 1.1 and PQM 1.2) installed on the HV busbar (2 MV PQMs at substation C were not measuring during this incident due to substation maintenance.)

From Table I it is concluded that method M1 cannot be applied to substation A because only one 11 kV busbar exists. When M1 is applied to substation B, it classifies the source of the dip incident to be within the upstream HV grid. M2 and M3 also assign the source of the dip incident to be within the HV grid.

Case Study 1 is an example where all 3 methods produce correct results. Method M1 cannot be applied to substation A, a constraint resulting from the specific grid topology.

B) Case Study 2

Case study 2 considers a different asymmetrical dip incident recorded in the network represented in Fig. 6. Results are listed in Table II.

PQM 3.10 recorded the lowest residual voltage value of 32.04 %. Dip durations were from 540 ms to 590 ms, with the largest difference in start time around 4 ms.

Again, M1 could only be applied to substation B. Both M1 and M2 incorrectly attribute the source of the dip incident as within the HV grid.

M3 correctly determines the root cause of the dip incident to be downstream of substation A. This result was manually confirmed by a detailed analysis of coherent measurements of reactive power, voltage, and current waveforms.

TABLE I
Case Study 1: Event data and results of the three localization methods

Substation and measurement device	**Residual voltage [%]**	**Duration [s]**	**Offset from first event [ms]**	**M1**	**M2**	**M3**
Sub A 3.10 (11 kV)	84.48	0.35	2	N/A (Only one MV busbar)	(4): True **Origin: HV grid**	(7*): True (8): True for all substations **Origin: HV grid**
Sub B 3.14 (11 kV)	83.27	0.36	2	(1): True (2): True (3): True **Origin: HV grid**		
Sub B 3.15 (11 kV)	83.20	0.36	2			
Sub B 3.16 (11 kV)	83.28	0.38	0			
1.1 (66 kV)	83.27	0.38	0			
1.2 (66 kV)	87.23	0.38	0			

TABLE II
Caste Study 2: Event data and results of the three localization methods

Substation and measurement device	**Residual voltage [%]**	**Duration [s]**	**Offset from first event [ms]**	**M1**	**M2**	**M3**
Sub A 3.10 (11 kV)	32.04	0.59	0	N/A (Only one MV busbar)	(4): True **Origin: HV grid**	(7*): True (8): False only for substation A **Origin: MV grid (substation A)**
Sub B 3.14 (11 kV)	87.59	0.54	4	(1): True (2): True (3): True **Origin: HV grid**		
Sub B 3.15 (11 kV)	87.56	0.54	4			
Sub B 3.16 (11 kV)	86.19	0.55	4			
1.1 (66 kV)	87.07	0.54	4	-	-	
1.2 (66 kV)	87.07	0.54	0	-	-	

This work is licensed under a Creative Commons Attribution 4.0 License. For more information, see https://creativecommons.org/licenses/by/4.0/

This article has been accepted for publication in IEEE Open Access Journal of Power and Energy. This is the author's version which has not been fully edited and content may change prior to final publication. Citation information: DOI 10.1109/OAJPE.2023.3268499

C) Case Study 3

Case study 3 includes substation C, whose MV busbars are monitored by two PQMs (3.30 and 3.32 in Fig. 6). The 66 kV supply to substations A, B and C are monitored by PQM 1.2.

Results are listed in Table III. The lowest residual voltage of 32.76 % was recorded by PQM 3.32 at substation C. The remaining MV PQMs recorded residual voltages between 89.02 % and 88.03 %. PQM 1.2 recorded at HV a residual voltage of 87.58 %. Event duration at the different PQMs ranges between 410 ms and 440 ms, with a maximum offset between events start time of 2 ms.

Again, M1 cannot be applied to substation A. M1 found the dip incident as having a location upstream of substation B but downstream of substation C.

M2 found the location of the voltage dip incident to be in the upstream HV grid.

M3, correctly, found the location of the voltage dip incident to be downstream and in the MV side of substation C, like M1.

D) Case Study 4

During case study 4 only one transformer monitored by PQM 3.30 was in service at substation C. For this case, substation C has therefore a configuration similar to substation A.

Results are listed in Table IV. This dip incident has a duration between 380 and 410 ms with a maximum time offset among the 6 dip events of 17 ms. The lowest residual voltage of 43.03 % was recorded at substation C with remaining residual voltages at MV side of the other substations recorded as between 81.84 % and 83.82 %. At HV, monitored by PQM 1.2, the residual voltage was 82.46 %.

In this case, M1 applied to substation B attributes the dip incident to have a location within the upstream HV grid.

M2 also identifies the source of the dip incident as upstream, within the HV grid.

M3 correctly reports the source of the voltage incident to be in the MV system downstream of the HV/MV transformer at substation C.

Observe that, whilst M3 has been implemented using the available measurements at HV level, i.e., applying criterion (7*) and equation (8), it could also be implemented using only the MV measurements by application of criterion (5*) and equation (6), that is considering the same data used for M1 and M2. In all the tested case studies, the final outcomes on the localization of the origin of the voltage event would be exactly the same, thus highlighting that M3 advantages with respect to M1 and M2 are kept even when the same measurements are considered.

TABLE III
Caste Study 3: Event data and results of the three localization methods

Substation and measurement device	**Residual voltage [%]**	**Duration [s]**	**Offset from first event [ms]**	**M1**	**M2**	**M3**
Sub A 3.10 (11 kV)	87.90	0.41	2	N/A (Only one MV busbar)	(4): True **Origin: HV grid**	(7*): True (8): False only for substation C, PQM 3.32 **Origin: MV grid (substation C, Downstream PQM 3.32)**
Sub B 3.14 (11 kV)	88.09	0.41	2	(1): True (2): True (3): True **Origin: HV grid**		
Sub B 3.15 (11 kV)	88.03	0.41	2			
Sub B 3.16 (11 kV)	87.83	0.41	2			
Sub C 3.30 (11 kV)	89.02	0.41	2	(1): False (2): True (3): False **Origin: MV grid**		
Sub C 3.32 (11 kV)	32.76	0.44	0			
1.2 (66 kV)	87.58	0.41	2	-	-	

TABLE IV
Caste Study 4: Event data and results of the three localization methods

Substation and measurement device	**Residual voltage [%]**	**Duration [s]**	**Offset from first event [ms]**	**M1**	**M2**	**M3**
Sub A 3.10 (11 kV)	83.82	0.38	17	N/A (Only one MV busbar)	(4): True **Origin: HV grid**	(7*): True (8): False only for substation C **Origin: MV grid (substation C)**
Sub B 3.14 (11 kV)	82.66	0.39	17	(1): True (2): True (3): True **Origin: HV grid**		
Sub B 3.15 (11 kV)	82.71	0.39	17			
Sub B 3.16 (11 kV)	81.84	0.39	13			
Sub C 3.30 (11 kV)	43.03	0.41	0	N/A (Only one MV busbar)		
1.2 (66 kV)	82.46	0.39	10	-	-	

This work is licensed under a Creative Commons Attribution 4.0 License. For more information, see https://creativecommons.org/licenses/by/4.0/

This article has been accepted for publication in IEEE Open Access Journal of Power and Energy. This is the author's version which has not been fully edited and content may change prior to final publication. Citation information: DOI 10.1109/OAJPE.2023.3268499

VI. CONCLUSION

An improved methodology has been presented to locate the source of a voltage dip as being in the HV or the MV network by making use of dip events recorded synchronously at different HV and MV sites in an interconnected HV/MV network. The pragmatic value of this method is by considering only the residual voltages and duration of each event. This allows a simple and straightforward application on coherent PQ data. An automated classification methodology can easily be derived from the principles presented and implemented as an efficient dip analysis tool.

The methodology presented was tested by means of case studies obtained from a commercial platform for analysing power quality events detected in the distribution grid located in South Africa. During the tests, the proposed methodology proved to outperform the methods used as a comparison, demonstrating the possibility of being easily implemented to improve the localisation of voltage dips sources.

REFERENCES

[1] X. Zheng, B. Wang, D. Kalathil and L. Xie, "Generative Adversarial Networks-Based Synthetic PMU Data Creation for Improved Event Classification", in *IEEE Open Access Journal of Power and Energy*, vol. 8, pp. 68-76, 2021.

[2] P. Castello, C. Muscas, P. A. Pegoraro, S. Sulis, "Active Phasor Data Concentrator performing adaptive management of latency", in *Sustainable Energy, Grids and Networks*, vol. 16, pp. 270-277, 2018.

[3] S. Rinaldi, P. Ferrari, A. Flammini, E. Sisinni and A. Vezzoli, "Uncertainty Analysis in Time Distribution Mechanisms for OMS Smart Meters: The Last-Mile Time Synchronization Issue", in *IEEE Transactions on Instrumentation and Measurement*, vol. 68, no. 3, pp. 693–703, March 2019.

[4] *IEEE/IEC International Standard* - Measuring relays and protection equipment - Part 118-1: Synchrophasor for power systems - Measurements," in *IEC/IEEE 60255-118-1:2018*, pp.1-78, 19 Dec. 2018

[5] C. Galvez and A. Abur, "Fault Location in Active Distribution Networks Containing Distributed Energy Resources (DERs)", in *IEEE Transactions on Power Delivery*, vol. 36, no. 5, pp. 3128-3139, 2021.

[6] P. Castello et al. "Integration of power quality and fault data into a PMU-based Wide Area Monitoring System", in *IEEE 11th Int. Workshop on Applied Measurement for Power Systems* (*AMPS*), 2021.

[7] P. A. Pegoraro, A. Meloni, L. Atzori, P. Castello and S. Sulis, "PMU-Based Distribution System State Estimation with Adaptive Accuracy Exploiting Local Decision Metrics and IoT Paradigm", in *IEEE Transactions on Instrumentation and Measurement*, vol. 66, no. 4, pp. 704-714, 2017.

[8] Y. Yuan, K. Dehghanpour and Z. Wang, "Mitigating Smart Meter Asynchrony Error Via Multi-Objective Low Rank Matrix Recovery", in *IEEE Transactions on Smart Grid*, vol. 12, no. 5, pp. 4308-4317, 2021.

[9] *IEC 61000-4-30:2015+AMD1:2021, Electromagnetic compatibility (EMC) - Part 4-30: Testing and measurement techniques - Power quality measurement methods,* 2021. Edition 3.1 (*IEC 61000-4-30:2015, ed. 3*).

[10] *IEEE recommended practice for power quality data interchange format (pqdif)*, IEEE Std 1159.3-2019 (Revision of IEEE Std 1159.3-2003).

[11] A. Monti, C. Muscas, and F. Ponci, "Phasor measurement units and wide area monitoring systems". Academic Press, 2016.

[12] *IEC/IEEE international standard - measuring relays and protection equipment - part 118-1: Synchrophasor for power systems - measurements*, IEC/IEEE 60255-118-1:2018, pp. 1–78, 2018.

[13] A. Moschitta, P. Carbone and C. Muscas, "Performance Comparison of Advanced Techniques for Voltage Dip Detection", in *IEEE Transactions on Instrumentation and Measurement*, vol. 61, no. 5, pp. 1494-1502, 2012.

[14] Y. Mohammadi, M. H. Moradi, R. C. Leborgne, "Locating the source of voltage sags: Full review, introduction of generalized methods and numerical simulations", in *Renewable and Sustainable Energy Reviews*, vol. 77, pp. 821-844, 2017.

[15] V. A. Katić and A. M. Stanisavljević, "Smart Detection of Voltage Dips Using Voltage Harmonics Footprint", in *IEEE Transactions on Industry Applications*, vol. 54, no. 5, pp. 5331-5342, 2018.

[16] F. O. Passos, J. M. de Carvalho Filho, R. C. Leborgne, P. M. da Silveira, P. F. Ribeiro, "An alternative approach to locating voltage sag source side at the point of common coupling based on power-flow information", in *Journal of Control, Automation and Electrical Systems*, 26(5), 579-587, 2015.

[17] R. C. Leborgne, D. Karlsson, "Voltage sag source location based on voltage measurements only", in *Electrical Power Quality and Utilisation. Journal*, *14*, 25-30, 2008.

[18] V. B. Núnez, J. M. Frigola, S. H. Jaramillo, J. S. Losada, "Evaluation of fault relative location algorithms using voltage sag data collected at 25-kV substations", in *European transactions on electrical power*, *20*(1), 34-51, 2010.

[19] S. Turizo, G. Ramos and D. Celeita, "Voltage Sags Characterization Using Fault Analysis and Deep Convolutional Neural Networks", in *IEEE Transactions on Industry Applications*, vol. 58, no. 3, pp. 3333-3341, May-June 2022.

[20] M. De Santis, C. Noce, P. Varilone, and P. Verde, "Analysis of the origin of measured voltage sags in interconnected networks", in *Electric Power Systems Research*, vol. 154, pp. 391–400, 2018.

[21] C. Noce, M. D. Santis, L. D. Stasio, P. Varilone and P. Verde, "Detecting the Origin of the Voltage Sags Measured in the Smart Grids", 2019 *International Conference on Clean Electrical Power* (ICCEP), pp. 129-135, 2019.

[22] P. Castello, C. Muscas, P. A. Pegoraro, S. Sulis, J. Rens and J. van Zyl, "Power Quality Data Platform for Analysis and Location of Voltage Dips: a Preliminary Study," *2022 20th International Conference on Harmonics & Quality of Power (ICHQP)*, 2022.

[23] Lennerhag, O., & Bollen, M. (2021). Power Quality. In Springer Handbook of Power Systems (pp. 1171-1203). Springer, Singapore

[24] "QuEEN, Qualità dell'Energia Elettrica": https://queen.rse-web.it/eng/home.aspx (Accessed 10 Sept. 2022).

[25] M. Zanoni, R. Chiumeo, L. Tenti, M. Volta, "Advanced Machine Learning Functionalities in the Medium Voltage Distributed Monitoring System QuEEN: A Macro-Regional Voltage Dips Severity Analysis", in *Energies*, 14, 7949, 2021.

[26] Sistema di monitoraggio nazionale della qualità della tensione alle semisbarre MT di cabina primaria: formato dei dati e individuazione dell'origine dei buchi di tensione per la trasmissione all'Autorità e la rendicontazione/visualizzazione dal sito web MonNaLiSA: https://www.arera.it/allegati/docs/17/012-17dieuall.pdf (Accessed 10 Sept. 2022).

This work is licensed under a Creative Commons Attribution 4.0 License. For more information, see https://creativecommons.org/licenses/by/4.0/